View metadata, citation and similar papers at core.ac.uk
brought to you by CORE
provided by Repository of the Academy's Library

# Comparison of Sigma-Point Filters for State Estimation of Diabetes Models

Péter Szalay*, Adrienn Molnár *, Márk Müller*, György Eigner†, Imre Rudas†,
Zoltán Benyó* and Levente Kovács†
*Department of Control Engineering and Information Technology
Budapest University of Technology and Economics, Budapest, Hungary
E-mail: szalaip@iit.bme.hu, molnar.adri89@gmail.com, muller.mark90@gmail.com, benyo@iit.bme.hu
†Institute of Information Systems, John von Neumann Faculty of Informatics
Obuda University, Budapest, Hungary
E-mail: eigner.gyorgy@phd.uni-obuda.hu, rudas@uni-obuda.hu, kovacs.levente@nik.uni-obuda.hu

***Abstract*—In physiological control there is a need to estimate signals that cannot be measured directly. Burdened by measurement noise and unknown disturbances this proves to be challenging, since the models are usually highly nonlinear. Sigma-point filters could represent an adequate choice to overcome this problem. The paper investigates the applicability of several different versions of sigma-point filters for the Artificial Pancreas problem on the widely used Cambridge (Hovorka)-model.**

## I. Introduction

In the human body glucose serves as the primary source of energy. The concentration of blood glucose is kept in a narrow range (3.9 - 7.8 mmol/L) by a complex endocrine system and insulin plays a key role in this process. When insulin secretion or insulin action is impaired, diabetes is diagnosed [1]. From engineering point of view the treatment of diabetes mellitus, and more specifically type-1 diabetes mellitus (T1DM), can be seen as a control problem. Artificial pancreas (AP) is a mean to solve this task in the clinical practice with an automated system that can replace the partially or totally deficient blood glucose regulation [2].

All closed-loop controllers require sensor, however the commercially available continuous glucose sensors are burdened with significant measurement noise [3]. Furthermore, the more sophisticated model-based control techniques require signals which are not available for measurement. Certain forms of model predictive control (MPC), which is one of the most commonly used methods for physiology-related control problems [4], [5], use information from all state variables of the state-space representation of the process. Nonlinear methods, such as exact linearization [6] usually have the same requirement. In the case of linear parameter varying (LPV) modeling or control, a set of time-varying parameters is needed to be available for measurement [7], [8]. It is needless to say that various other control methods could benefit from more information regarding the behavior of the controlled process.

Model-based filters can satisfy such demands. In the case of significant measurement noise and large unknown disturbances (for AP i.e. meal intake, physical activity), Kalman filter is usually preferred [9]. In this paper the applicability of several different versions of Kalman filters will be investigated.

## II. The T1DM Model

The investigated model is based on the one presented by [4], which is described by 11 nonlinear differential equations [8], and contains time-varying parameters. However, in this work a reduced 6th order model is used, with no parameters changing in time. This is necessary because modeling time-dependent variables is not a trivial task, and not in the scope of this paper. Furthermore, the neglected state variables would introduce time constants comparable to the sampling time of the sensor. The used model is described by the following equations:

$$\begin{aligned}
\dot{Q}_1(t) &= -\left(\tfrac{F_{01}}{Q_1(t)+V_G} + x_1(t)\right) Q_1(t) + k_{12}Q_2(t) - \\
&-R_{cl}max\{0, Q_1(t) - R_{thr}V_G\} - Phy(t) + \\
&+EGP_0max\{0, 1 - S_{IE}\tfrac{k_a}{V_I k_e}S_2(t)\} + \\
&+min\left\{U_{G,ceil}, \tfrac{G_1(t)}{t_{max}}\right\} \\
\dot{Q}_2(t) &= x_1(t)Q_1(t) - \left(k_{12} + S_{ID}\tfrac{k_a}{V_I k_e}S_2(t)\right)Q_2(t) \\
\dot{x}_1(t) &= -k_{b1}x_1(t) + S_{IT}k_{b1}\tfrac{k_a}{V_I k_e}S_2(t) \\
\dot{S}_2(t) &= -k_a S_2(t) + k_a S_1(t) \\
\dot{S}_1(t) &= -k_a S_1(t) + u(t) \\
\dot{G}_1(t) &= -\frac{G_1(t)}{max\left\{t_{max}, \tfrac{G_1(t)}{U_{G,ceil}}\right\}} + D(t)
\end{aligned} \tag{1}$$

where the state variables are: the $Q_1$ and $Q_2$ amount of glucose in accessible and non-accessible compartments [mmol], the $x_1$ remote effect of insulin on glucose distribution [1/min], the $S_1$ and $S_2$ insulin masses in the accessible and non-accessible compartments [mU], the $G_1$ glucose mass in the accessible and non-accessible compartments related to glucose absorption [mmol]. $u$ injected insulin flow of rapid-acting insulin [mU/min] is the input of the system, while the $D$ amount of ingested carbohydrates [mmol/min], and $Phy$ effect of physical activity [mmol/min] are considered as disturbances. The description of the model parameters can be found in [4].

The system output is the glucose concentration in the accessible compartment $\frac{Q_1}{V_G}$. Glucose measurements are available every 5 minutes by continuous glucose measurement sensors (CGMS). The applied sensor model is without lag time, and the measurement noise is assumed to be additive white noise with

978-1-4799-3840-7/14/$31.00 ©2014 IEEE

1 $mmol^2/L^2$ variance. A more sophisticated approach would be to use smaller additive noise, but include sensor drift and the transfer within the subcutaneous compartments.

The model (1) can be approximated in discrete time using four step Runge-Kutta method: $\mathrm{x}_{k+1} = \mathrm{f}(\mathrm{x}_k, \mathrm{u}_k, \mathrm{w}_k)$, $y_k = \mathrm{C}\mathrm{x}_k + n_k$, where $\mathrm{x}_k \in \mathbb{R}^{n_x}$ is the vector of state variables, $y_k \in \mathbb{R}$ denotes the measured output disturbed with $n_k \sim \mathcal{N}(0, R_k)$ additive white noise. $\mathrm{u}_k \in \mathbb{R}^{n_u}$ is the vector of known deterministic inputs, while $\mathrm{w}_k \sim \mathcal{N}(0, \mathbf{Q}_k)$ is the vector of disturbances affecting the states, with assumingly zero mean Gaussian distribution and $n_w \times n_w$ real positive semidefinite covariance matrix $\mathbf{Q}_k$. $\mathrm{f} : \mathbb{R}^{n_x} \times \mathbb{R}^{n_u} \times \mathbb{R}^{n_w} \to \mathbb{R}^{n_x}$ is a piecewise continuous nonlinear mapping, while vector C defines a linear mapping. In the case of model (1) $n_x = 6$ and $n_w = 2$. The number of measured outputs is one, as well as the dimension of the measurement noise and the deterministic input.

## III. Sigma-Point Filters

One of the most widely used nonlinear Kalman filter up to date is still the Extended Kalman Filter (EKF), which is based on first-order linearization of the nonlinear models. This approach may fail when the system contains high nonlinearities, large disturbances or initial estimation errors [9]. The need to improve EKF gave birth to Sigma-point filters. They can be seen as a form of nonlinear Kalman filters which use a number of deterministic samples, called sigma-points, to represent the probability distribution of the system state [10]. There are several versions which differ mainly on how these sigma-points are selected. Cubature Kalman Filter (CKF) is based one the Cubature rule [11] and is one of the most straightforward approaches. The slightly more popular Unscented Kalman Filter (UKF) relies on the Unscented Transformation [10] with parameters that can be tuned for each filtering problem in order to achieve better performance. When Gaussian distribution is guaranteed Gauss-Hermite Quadrature Filter (GHKF) offers the highest accuracy [12]. However, it also requires a large amount of sigma-points and hence increased computational power which can be undesirable in certain practical applications. Sparse-grid quadrature nonlinear filtering (SGQF) can overcome this curse of dimensionality problem [13]. Furthermore, CKF and UKF can be considered as a special form of SGQF.

### A. Sigma-point selection

Let us introduce the notation $\chi$ for a set of sigma-points. This set contains $N$ sigma points denoted as $\xi_i$, $i = 1, \ldots, N$. The sigma-points represent the stochastic variable $\mu$ with $\hat{\mu}$ mean and $\mathbf{\Sigma}$ covariance matrix, and can be written in the following form:

$$\xi_i = \mathbf{\Sigma}^{\frac{1}{2}} \varphi_i + \hat{\mu} \tag{2}$$

$\Sigma^{\frac{1}{2}}$ is the factor of $\mathbf{\Sigma}$ so that $\mathbf{\Sigma} = \mathbf{\Sigma}^{\frac{1}{2}} \mathbf{\Sigma}^{\frac{T}{2}}$, and since $\mathbf{\Sigma}$ is positive definite, Cholesky decomposition is commonly used. In case $\mathbf{\Sigma}$ is close to being singular, or non-definite due to sigma point collapse [14], singular value decomposition can be used as well [13]. $\mu$ is not limited to state variables only, it can contain the disturbances and measurement noises as well [15], so that:

$$\hat{\mu} = \begin{pmatrix} \hat{\mathrm{x}} \\ 0 \\ 0 \end{pmatrix} \quad \mathbf{\Sigma} = \begin{bmatrix} \Sigma & 0 & 0 \\ 0 & \mathbf{Q} & 0 \\ 0 & 0 & R \end{bmatrix} \tag{3}$$

where $\mathbf{Q}$ and $R$ denote covariance matrices of the disturbances and measurement noise, just like earlier. Using these sigma points one can estimate the mean and covariance of the distribution of $f(\chi)$ as a weighted sum, where $f(.)$ is a nonlinear function:

$$\begin{aligned} \mathrm{E}\{f(\mu)\} = \bar{\mathrm{f}}_\mu \approx \sum_{i=1}^{N} \omega_i^{(m)} f(\xi_i) \\ cov\{f(\mu)\} \approx \sum_{i=1}^{N} \omega_i^{(c)} \left( (f(\xi_i) - \bar{\mathrm{f}}_\mu)(f(\xi_i) - \bar{\mathrm{f}}_\mu)^T \right) \end{aligned} \tag{4}$$

There are various strategies to choose $\varphi_i$ and the weights $\omega_i^{(m)}$ and $\omega_i^{(c)}$. In case or CKF there are $2L$ sigma-points, where $L$ is the dimension of $\mu$. The weights and basis functions $\omega^{(m)}$, $\omega^{(c)}$ and $\varphi$ in the case of a CKF are:

$$\begin{aligned} \varphi_i &= \begin{cases} \mathrm{e}_i \sqrt{L} & i = 1, \ldots, L \\ -\mathrm{e}_i \sqrt{L} & i = L+1, \ldots, 2L \end{cases} \\ \omega_i^{(m)} &= \omega_i^{(c)} = \tfrac{1}{\sqrt{L}} \end{aligned} \tag{5}$$

where $\mathrm{e}_i$ denotes the unit vector in $\mathbb{R}^L$ with the $(i-1)$th element being 1. Note that CKF does not have any adjustable parameter, opposed to UKF which has three: $\kappa$, $\alpha$ and $\beta$. The weights and basis functions $\omega$ and $\phi$ in the case of a CKF are:

$$\begin{aligned} \varphi_i &= \begin{cases} 0 & i = 1 \\ \mathrm{e}_i \sqrt{L+\lambda} & i = 2, \ldots, L+1 \\ -\mathrm{e}_i \sqrt{L+\lambda} & i = L+2, \ldots, 2L+1 \end{cases} \\ \omega_i^{(m)} &= \begin{cases} \frac{\lambda}{n+\lambda} & i = 1 \\ \omega_i^{(m)} = \frac{1}{2(n+\lambda)} & i = 2, \ldots, 2L+1 \end{cases} \\ \omega_1^{(c)} &= \begin{cases} \frac{\lambda}{n+\lambda} + 1 - \alpha^2 + \beta & i = 1 \\ \omega_i^{(c)} = \frac{1}{2(n+\lambda)} & i = 2, \ldots, 2L+1 \end{cases} \end{aligned} \tag{6}$$

where $\lambda = \alpha^2(L + \kappa) - L$ is a scaling parameter [9]. The constant $\alpha$ determines the spread of sigma points around $\mu$, and is usually set to a small positive value (e.g. $1 \geq \alpha \geq 10^{-4}$). The constant $\kappa$ is a second scaling parameter usually set to $3 - L$ so that the kurtosis of the sigma-points agrees with that of the Gaussian distribution [16]. $\beta$ is used to incorporate prior knowledge of the distribution of $\mu$ and usually set to 2 for Gaussian distribution. In case $\alpha = 1$ and $\beta = 0$ both CKF and UKF can be seen as a special case of level-2 SGQF.

The level-3 SGQF requires $2L^2 + 4L + 1$ or less sigma-points. The exact number depends on how the three free parameters – $p_1$, $p_2$ and $p_3$ – are chosen. Similarly to the GHKF, these parameters are selected from the perspective of an univariate estimation, where the points $\mu + \{-p_1, 0, p_1\}$ and $\mu + \{-p_3, -p_2, 0, p_2, p_3\}$ are used to estimate certain moments of an univariate Gaussian distribution transformed by a nonlinear function. If all parameters are different, the sigma-points used in the level-3 SGQF are shown in equation (7), where $C = L(L-1)/2$, while $\hat{\omega}_1, \ldots, \hat{\omega}_5$ are defined from

$$\varphi_i = \left\{ \begin{array}{cc} 0 \quad i=1 & \frac{(L-1)(L-2+L\hat{\omega}_1^2)}{2} - L(L-1)\hat{\omega}_1 + L\hat{\omega}_3 \\ \mathrm{e}_i p_1 \quad i=2,\ldots,L+1 & \} (L-1)\hat{\omega}_2(\hat{\omega}_1 - 1) \\ -\mathrm{e}_i p_1 \quad i=L+2,\ldots,2L+1 & \\ \mathrm{e}_i p_2 \quad i=2L+2,\ldots,3L+1 & \} \hat{\omega}_4 \\ -\mathrm{e}_i p_2 \quad i=3L+2,\ldots,4L+1 & \\ \mathrm{e}_i p_3 \quad i=4L+2,\ldots,5L+1 & \} \hat{\omega}_5 \\ -\mathrm{e}_i p_3 \quad i=5L+2,\ldots,6L+1 & \\ \mathrm{e}_i p_1 + \mathrm{e}_j p_1 \quad i=6L+2,\ldots,6L+1+C & \\ -\mathrm{e}_i p_1 + \mathrm{e}_j p_1 \quad i=6L+2+C,\ldots,6L+1+2C & \\ \mathrm{e}_i p_1 - \mathrm{e}_j p_1 \quad i=6L+2+2C,\ldots,6L+1+3C & \\ -\mathrm{e}_i p_1 - \mathrm{e}_j p_1 \quad i=6L+2+3C,\ldots,6L+1+4C & \end{array} \right\} = \omega_i^{(m)} \quad (7)$$

the parameters $p_1, p_2, p_3$ using moment matching method. Furthermore, $\omega_i^{(c)} = \omega_i^{(m)}$ and $j \neq i$.

The standard algorithm ( [9]) is as follows:

*1) Initialization:* The initial estimation of the $\hat{\mathrm{x}}_0$ state variables and the $\chi_0$ initial sigma points are determined using $\mathbf{\Sigma}_0$, $\mathbf{Q}_0$ and $\mathbf{R}_0$. The latter two are only embedded into the sigma points if the disturbances or measurement noises are not linear and additive. In the case of embedding, $\chi_k$ can be divided to $\left[ \begin{array}{ccc} \chi_k^{(\hat{x})T} & \chi_k^{(w)T} & \chi_k^{(n)T} \end{array} \right]^T$ for all $k$.

*2) Estimation:*

1) Propagate the sigma points through the nonlinear function of the system
$$\chi_k^{(x)} = \mathrm{f}(\chi_{k-1}^{(\hat{x})}, \chi_{k-1}^{(w)}) \quad (8)$$
2) Let the weighted mean of the propagated sigma points be our initial estimation of the state vector. If $\chi_k^{(x)} = [\xi_{k,1}^{(x)}, \ldots, \xi_{k,N}^{(x)}]$ the result will be:
$$\bar{\mathrm{x}}_k = \sum_{i=1}^{N} \omega_i^{(m)} \xi_{k,i}^{(x)} \quad (9)$$
3) The covariance matrix of the state variables is estimated as follows:
$$\begin{array}{l} \mathbf{p}_{xx,i} = (\xi_{k,i}^{(x)} - \bar{\mathrm{x}}_k)(\xi_{k,i}^{(x)} - \bar{\mathrm{x}}_k)^T \\ \mathbf{P}_k^{(xx)} = \mathbf{Q}_k + \sum_{i=1}^{N} \omega_i^{(c)} \mathbf{p}_{xx,i} \end{array} \quad (10)$$
$\mathbf{Q}_k$ is only added, if the disturbance $\mathrm{w}_k$ is not embedded to the sigma points.
4) Let us propagate the transformed sigma points to the output.
$$\chi_k^{(y)} = \mathrm{C}\chi_k^{(x)} + \chi_{k-1}^{(n)} \quad (11)$$
$\chi_{k-1}^{(n)}$ is neglected, unless it is embedded into the sigma points.
5) Let the weighted mean of the propagated sigma points be our initial estimation of the measured output. If $\chi_k^{(y)} = [\xi_{k,1}^{(y)}, \ldots, \xi_{k,N}^{(y)}]$ the result will be:
$$\bar{y}_k = \sum_{i=1}^{N} \omega_i^{(m)} \xi_{k,i}^{(y)} \quad (12)$$
6) The covariance matrix of the output and the cross-covariance between the output and the states are estimated as follows:
$$\begin{array}{l} p_{yy,i} = (\xi_{k,i}^{(y)} - \bar{y}_k)(\xi_{k,i}^{(y)} - \bar{y}_k)^T \\ P_k^{(yy)} = R_k + \sum_{i=1}^{N} \omega_i^{(c)} p_{yy,i} \\ \mathrm{p}_{xy,i} = (\xi_{k,i}^{(x)} - \bar{\mathrm{x}}_k)(\xi_{k,i}^{(y)} - \bar{y}_k)^T \\ \mathrm{P}_k^{(xy)} = \sum_{i=1}^{N} \omega_i^{(c)} \mathrm{p}_{xy,i} \end{array} \quad (13)$$
$R_k$ is only added, if the measurement noise $n_k$ is not embedded into the sigma points.

*3) Update:*

1) The state estimation is updated using the difference between the estimated and the actual measured output
$$\hat{\mathrm{x}}_k = \bar{\mathrm{x}}_k + \mathrm{K}_k(y_k - \bar{y}_k) \quad (14)$$
where the Kalman gain $\mathrm{K}_k$ is computed using the covariance anc cross-covariance matrices:
$$\mathrm{K}_k = \mathrm{P}_k^{(xy)} \left( P_k^{(yy)} \right)^{-1} \quad (15)$$
2) The estimation error covariance matrix is updated as follows:
$$\mathbf{\Sigma}_k = \mathbf{P}_k^{(xx)} - \mathrm{K}_k P_k^{(yy)} \mathrm{K}_k^T \quad (16)$$
3) The sigma point set $\chi_k$ is computed using (2).

### B. Square-root filtering

If the number of sigma points used is not too large, it is possible to increase the numerical robustness of the filter algorithm by avoiding the factorization and computing the factor $\mathbf{\Sigma}_k^{\frac{1}{2}}$ directly. This is referred to as square-root filtering. In this work the method presented in [15] will be used. This approach requires $\mathrm{w}_k$ and $n_k$ to be embedded into the sigma points, furthermore all of the weights $\omega^{(c)}$ to be non-negative. The classical algorithm remains mostly unchanged except for (10), (13), (15) and (16). These will be substituted with the followings:

$$\mathbf{P}_k^{(x)} = \sum_{i=1}^{N} \sqrt{\omega_i^{(c)}}(\xi_{k,i}^{(x)} - \bar{\mathrm{x}}_k) \tag{17}$$

$$\mathrm{P}_k^{(y)} = \sum_{i=1}^{N} \sqrt{\omega_i^{(c)}}(\xi_{k,i}^{(y)} - \bar{y}_k) \tag{18}$$

$$\begin{bmatrix} \tilde{P}_k^{(yy)} & 0 & 0 \\ \tilde{\mathrm{P}}_k^{(xy)} & \mathbf{\Sigma}_k^{\frac{1}{2}} & 0 \end{bmatrix} = Triang\left\{ \begin{bmatrix} \mathrm{P}_k^{(y)} \\ \mathbf{P}_k^{(x)} \end{bmatrix} \right\} \tag{19}$$

$$\mathbf{K}_k = \tilde{\mathrm{P}}_k^{(xy)} \left( \tilde{P}_k^{(yy)} \right)^{-1} \tag{20}$$

where *Triang* refers to the transpose of the upper triangular result $\mathbf{\Gamma}$ of the QR decomposition of the transposed matrix (21). Note, that the unitary matrix $\mathbf{\Theta}$ resulting from the decomposition is not used, hence does not need to be computed.

$$\begin{aligned} \mathbf{\Gamma}^T &= Triang\{\mathbf{A}\} \\ \mathbf{\Theta\Gamma} &= QR\{\mathbf{A}^T\} \end{aligned} \tag{21}$$

### C. $\mathcal{H}_\infty$ filtering

There is little information available of the noise statistics in practice. Hence, one can improve the estimation accuracy by making the filter either adaptive or robust. $\mathcal{H}_\infty$ filter is a good example for the latter. We can define $\mathrm{z}_k = \mathbf{L}_k \mathrm{x}_k$ signal which we wish to estimate ($\hat{\mathrm{z}}_k$). The aim is to minimize the estimation error in the worst case of the disturbances and uncertainties by minimizing the following cost function [17], [18]:

$$J_k = \frac{\sum_{j=0}^{k} \|\hat{\mathrm{z}}_j - \mathbf{L}_j \mathrm{x}_j\|^2}{\|\tilde{\mathrm{x}}_0\|^2_{\Sigma_0^{-1}} + \sum_{j=0}^{k-1} \|\mathrm{w}_j\|^2_{\mathbf{Q}_j^{-1}} + \sum_{j=0}^{k} \|n_j\|^2_{R_j^{-1}}} \tag{22}$$

where $\tilde{\mathrm{x}}_0 = \mathrm{x}_0 - \hat{\mathrm{x}}_0$, the notation $\|\mathrm{x}\|^2_{\mathbf{P}}$ is defined as $\mathrm{x}^T\mathbf{P}\mathrm{x}$ and the assumption is that $\sum_{k=0}^{\infty} \mathrm{w}_k^T \mathrm{w}_k < \infty$ and $\sum_{k=0}^{\infty} n_k^2 < \infty$. $\hat{\mathrm{z}}_k$ is calculated to satisfy the condition $supJ < \gamma^2$, where *sup* stands for the supremum and $\gamma$ is a pre-defined positive scalar. One way to achieve this is to add virtual measurements to the existing ones, which will not be embedded:

$$\mathrm{y}_k^{(e)} = \begin{pmatrix} y_k \\ \mathrm{z}_k \end{pmatrix} = \begin{bmatrix} \mathrm{C} \\ \mathbf{L}_k \end{bmatrix} \mathrm{x}_k + \mathrm{n}_k^{(e)} \tag{23}$$

where the covariance matrix of the $\mathrm{n}_k^{(e)}$ extended measurement noise is:

$$\begin{bmatrix} R_k & 0 \\ 0 & -\gamma^2 I_{n_e} \end{bmatrix} \tag{24}$$

where $I_{n_e}$ is an $n_e \times n_e$ identity matrix and $n_e$ is the length of $\mathrm{z}_k$. Needless to say this is not an actual covariance matrix, because it is not positive definite. Using these extended measurements the classical algorithm needs to be modified at step (16) as follows:

$$\mathbf{\Sigma}_k = \mathbf{P}_k^{(xx)} - \mathbf{P}_k^{(xy^{(e)})} \left( \mathbf{P}_k^{(y^{(e)}y^{(e)})} \right)^{-1} \left( \mathbf{P}_k^{(xy^{(e)})} \right)^T \tag{25}$$

where $\mathbf{P}_k^{(y^{(e)}y^{(e)})}$ is the covariance matrix of the extended measurements and $\mathbf{P}_k^{(xy^{(e)})}$ is the cross-covariance between the extended measurements and the states. $\gamma$ is chosen so that $\mathbf{\Sigma}_k$ remains positive definite. In the case of $\mathcal{H}_\infty$ requirements square-root filtering is not possible.

## IV. Results

In this section results of the state estimation of the model (1) will be presented. The estimation capabilities were evaluated using 500 simulations lasting 48 hours with randomized inputs, measurement noise and initial estimation [19]. Moreover, the numerical values of the model parameters were randomly chosen from the 6 patient parameter sets presented in [4] and 50 virtual patient parameter sets generated using the parameter bounds also presented in [4]. To examine the accuracy of state estimation the following functions were used:

1) Average root-mean-square error (RMSE). For the $j$-th state variable and $N$ simulations consisting of $M$ samples each:

$$R_1^{(x_j)} = \frac{1}{N} \sum_{i=1}^{N} \sqrt{\frac{1}{M} \sum_{k=0}^{M} \left( x_j^{(i)}[k] - \hat{x}_j^{(i)}[k] \right)^2} \tag{26}$$

2) Maximum root-mean-square error based on $N$ simulations:

$$R_2^{(x_j)} = \max_i \sqrt{\frac{1}{M} \sum_{k=0}^{M} \left( x_j^{(i)}[k] - \hat{x}_j^{(i)}[k] \right)^2} \tag{27}$$

3) RMSE as a function of time, averaged over the simulation:

$$R_3^{(x_j)}[k] = \sqrt{\frac{1}{N} \sum_{i=1}^{N} \left( x_j^{(i)}[k] - \hat{x}_j^{(i)}[k] \right)^2} \tag{28}$$

4) A function capturing the trends in RMSE:

$$R_4^{(x_j)}[k] = \frac{1}{N} \sum_{i=1}^{N} \sqrt{\frac{1}{k} \sum_{l=0}^{k} \left( x_j^{(i)}[l] - \hat{x}_j^{(i)}[l] \right)^2} \tag{29}$$

Note that in previous sections the time step was denoted with a lower left index, but in this section square brackets are used. Out of the six state variables of (1) only three will be examined: $Q_1$, $Q_2$ and $G_1$. The variable $G_1$ is normalized to $G_1/t_{max}$. The first two are important for Linear Parameter Varying (LPV) control [8], while the third signal is basically an estimation of the most significant disturbance in blood glucose control: glucose absorbed from meal intake. The initial estimation error of the state variables is assumed to be less than 20 %. Usually in clinical practice there is enough time to let the initial transients of the filter to dissipate. It is more important for the filter to compensate the effect of the disturbances.

First, the three investigated filter in their classical form were compared: CKF, UKF and SGQF. EKF was included for comparison. For UKF the parameters $\kappa = 3 - L$, $\alpha = 1$ and $\beta = 2$ were used. For the SGQF the parameters were chosen as $p_1 = \sqrt{(3)}$, $p_2 = 1.36$ and $p_3 = \sqrt{L}$. Parameter

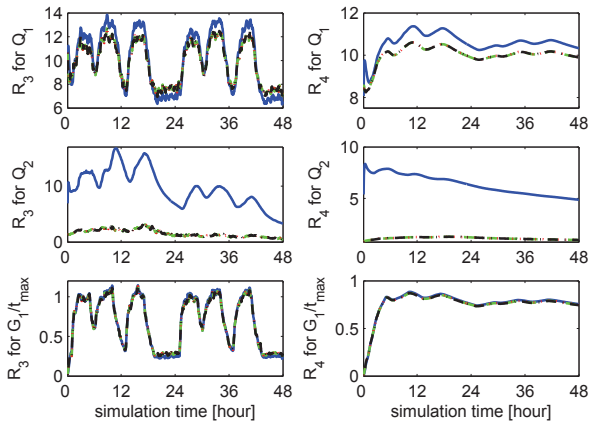


Fig. 1. Estimation results of standard filters: EKF - solid line, CKF - dashed line, UKF - dotted line, SQKF - dash-dotted line

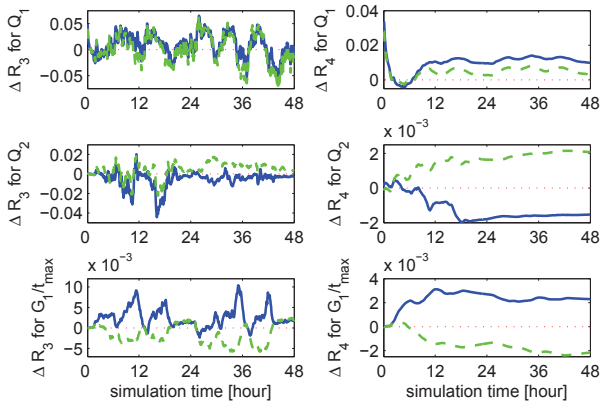


Fig. 2. Estimation results of standard filters relative to CKF: CKF - dotted line, UKF - solid line, SQKF - dashed line

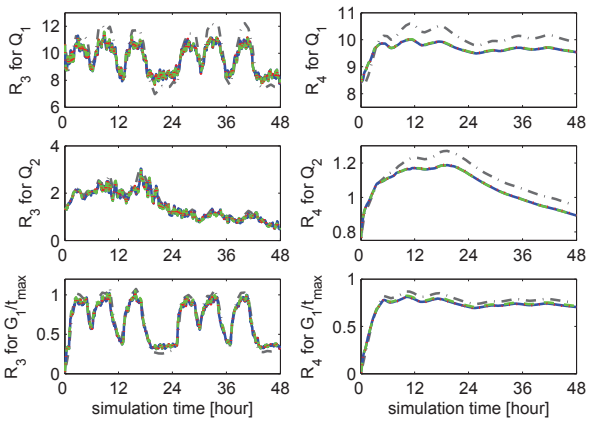


Fig. 3. Estimation results when assuming higher meal intake. CKF - solid line, UKF - dashed line, SQKF - dotted line, original CKF - dash-dotted line

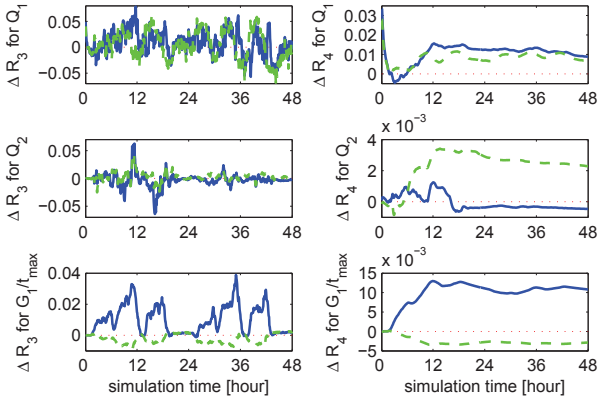


Fig. 4. Estimation results when assuming higher meal intake when the result for CKF is subtracted. CKF - dotted line, UKF - solid line, SQKF - dashed line

sensitivity of these filters was not investigated in this work. The results are presented in Figure 1. It is easy to confirm that all three sigma-point filters outperform the EKF. However, the difference between sigma-point filters is difficult to determine; hence, Figure 2 shows the results when the $R_3[k]$ and $R_4[k]$ functions of the CKF are subtracted from each other filter. It would seem that for each filter there is a state variable where they perform better than the other two.

It is visible on Figure 1 that each filter reacts slowly to the effect of the disturbance. Therefore, it was investigated whether assuming higher variance for the meal intake disturbance can result in better estimation. Figure 3 presents the acquired results. The original CKF is displayed with dash-dotted line for comparison. It is easy to see that the estimation error for $Q_1$ is smaller when meal intake occurs, but larger otherwise. Please refer to [8] regarding meal timing during the simulations. The reason is that the Kalman gain (15) will cause stronger correction in the update phase when the disturbance is higher compared to the measurement noise. On the other hand, larger gain will amplify the effect of the measurement noise on the estimation. Similarly to Figure 2 the performance of the filters relative to CKF is shown on Figure 4.

For the next comparison CKF, UKF and SGQF filters were modified into $\mathcal{H}_\infty$ filters based on [17]. The resulting estimation errors are displayed on Figure 5 relative to the original CKF for easier evaluation. The results suggest that $\mathcal{H}_\infty$ filtering can improve the results for the state variable $Q_2$, but there is only little benefit considering the other two estimated signals. To compare the $\mathcal{H}_\infty$ filters more effectively the results relative to $\mathcal{H}_\infty$ CKF are presented on Figure 6.

The average and maximum RMSE ($R_1$ and $R_2$) for all filters are summarized in Table I.

## V. Conclusion

The performance of three different sigma-point filters, with and without $\mathcal{H}_\infty$ filtering were evaluated and compared based on the estimation of selected state variables of a widely used nonlinear T1DM model.

Based on the acquired results it can be concluded that the sigma-point filters offer higher accuracy in this particular problem than EKF. Moreover, $\mathcal{H}_\infty$ filtering can improve these results even further. However, there was only little difference between the three filters: CKF, UKF and SQKF. One can

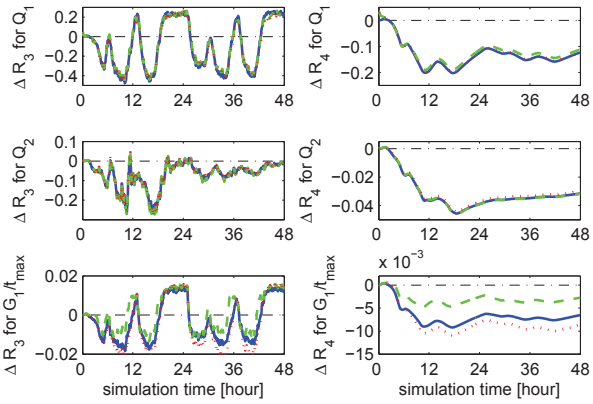


Fig. 5. Estimation results in the case of $\mathcal{H}_\infty$ filtering compapred to regular CKF. CKF - solid line, UKF - dashed line, SQKF - dotted line, original CKF - dash-dotted line

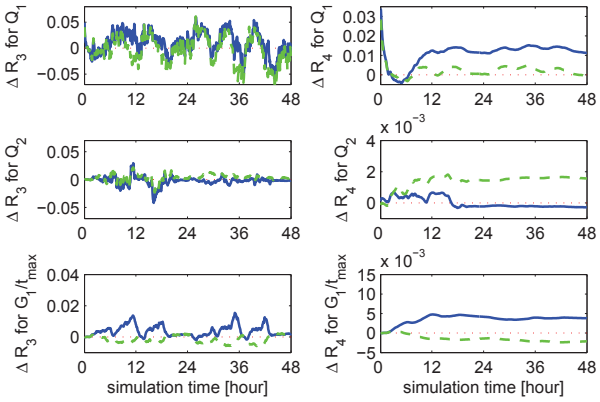


Fig. 6. Estimation results in the case of $\mathcal{H}_\infty$ filtering when the results for CKF are subtracted. CKF - dotted line, UKF - solid line, SQKF - dashed line

TABLE I. AVERAGED RMSE AND THE WORST CASE ERROR OF DIFFERENT FILTERS

| Filter | | Regular | | Large meal | | $\mathcal{H}_\infty$ filtering | |
|---|---|---|---|---|---|---|---|
| | | $R_1$ | $R_2$ | $R_1$ | $R_2$ | $R_1$ | $R_2$ |
| CKF | $Q_1$ | 9.89 | 12.21 | 9.54 | 11.62 | 9.77 | 12.00 |
| | $Q_2$ | 0.95 | 1.00 | 0.89 | 0.96 | 0.92 | 0.94 |
| | $G_1$ | 0.75 | 0.85 | 0.70 | 0.80 | 0.74 | 0.84 |
| UKF | $Q_1$ | 9.90 | 12.22 | 9.55 | 11.64 | 9.78 | 12.01 |
| | $Q_2$ | 0.95 | 1.03 | 0.89 | 0.91 | 0.92 | 0.95 |
| | $G_1$ | 0.75 | 0.85 | 0.72 | 0.81 | 0.74 | 0.85 |
| SQKF | $Q_1$ | 9.89 | 12.21 | 9.54 | 11.62 | 9.77 | 12.00 |
| | $Q_2$ | 0.95 | 0.97 | 0.90 | 0.91 | 0.92 | 1.01 |
| | $G_1$ | 0.74 | 0.85 | 0.70 | 0.80 | 0.74 | 0.84 |

choose one over the other based on other factors, such as number of sigma points required or possibility of square-root filtering. Our recommendation for this particular estimation problem is $\mathcal{H}_\infty$ SQKF for highest accuracy, and regular CKF for highest numerical robustness. Further work will focus on filters for prediction as input for a supervisory unit, but also more exact formulation of the problem can be assumed by fractional-order modeling and control aspects [20], [21].

## ACKNOWLEDGMENT

L. Kovacs is Bolyai Fellow of the Hungarian Academy of Sciences. The work was supported by the Hungarian GOP-1.1.1.-11-2012-0055 project, the Hungarian National Scientific Research Foundation Grant No. CK80316, and by the European Union TAMOP-4.2.2.A-11/1/KONV-2012-0073 project.

## REFERENCES

[1] A. Fonyó and E. Ligeti, *Physiology (in Hungarian)*, 3rd ed. Budapest, Hungary: Medicina, 2008.

[2] C. Cobelli, E. Renard, and B. Kovatchev, "Artificial pancreas: Past, present and future," *Diabetes*, vol. 60, no. 11, pp. 2672–2682, 2011.

[3] T. Battelino and J. Bolinder, "Clinical use of real-time continuous glucose monitoring," *Curr Diabetes Rev*, vol. 4, pp. 218–222, 2008.

[4] M. Wilinska, L. Chassin, C. Acerini, J. Allen, D. Dunger, and R. Hovorka, "Simulation environment to evaluate closed-loop insulin delivery systems in type 1 diabetes," *J Diab Sci Techn*, vol. 4, no. 1, pp. 132–144, 2010.

[5] L. Magni, D. M. Raimondo, C. D. Man, G. D. Nicolao, B. Kovatchev, and C. Cobelli, "Model predictive control of glucose concentration in type 1 diabetic patients: An in silico trial," *Biomed Sign Proc Contr*, pp. 338–346, 2009.

[6] P. Palumbo, P. Pepe, S. Panunzi, and A. De Gaetano, "Observer-based closed-loop control for the glucose-insulin system: Local input-to-state stability with respect to unknown meal disturbances," in *in Proc. American Control Conference (ACC), 2013*, 2013, pp. 1751–1756.

[7] R. S. Pena, A. Ghersin, and F. Bianchi, "Time-varying procedures for insulin-dependent diabetes mellitus control," *J Electr Comp Eng*, vol. 2011, pp. 1–10, 2011.

[8] P. Szalay, G. Eigner, M. Kozlovszky, I. Rudas, and L. Kovacs, "The significance of LPV modeling of a widely used T1DM model," in *Engineering in Medicine and Biology Society (EMBC), 2013 35th Annual International Conference of the IEEE*, 2013, pp. 3531–3534.

[9] S.Haykin, *Kalman Filtering and Neural Networks*. New York, USA.: John Wiley & Sons, Inc., 2002.

[10] S. Julier and J. Uhlmann, "Unscented filtering and nonlinear estimation," *Proceedings of the IEEE*, vol. 92, no. 3, pp. 401–422, 2004.

[11] I. Arasaratnam and S. Haykin, "Cubature kalman filters," *Automatic Control, IEEE Transactions on*, vol. 54, no. 6, pp. 1254–1269, 2009.

[12] I. Arasaratnam, S. Haykin, and R. Elliott, "Discrete-time nonlinear filtering algorithms using gauss–hermite quadrature," *Proceedings of the IEEE*, vol. 95, no. 5, pp. 953–977, 2007.

[13] B. Jia, M. Xin, and Y. Cheng, "Sparse-grid quadrature nonlinear filtering," *Automatica*, vol. 48, no. 2, pp. 327–341, 2012.

[14] R. Turner and C. Rasmussen, "Model based learning of sigma points in unscented kalman filtering," in *Machine Learning for Signal Processing (MLSP), 2010 IEEE International Workshop on*, 2010, pp. 178–183.

[15] M. Rutten, "Square-root unscented filtering and smoothing," in *Intelligent Sensors, Sensor Networks and Information Processing, 2013 IEEE Eighth International Conference on*, 2013, pp. 294–299.

[16] S. Julier, J. Uhlmann, and H. Durrant-Whyte, "A new approach for filtering nonlinear systems," in *American Control Conference, Proceedings of the 1995*, vol. 3, 1995, pp. 1628–1632 vol.3.

[17] B. Jia and M. Xin, "Sparse-grid quadrature $\mathcal{H}_\infty$ filter for discrete-time systems with uncertain noise statistics," *Aerospace and Electronic Systems, IEEE Transactions on*, vol. 49, no. 3, pp. 1626–1636, 2013.

[18] D. Simon, *Optimal State Estimation: Kalman, $\mathcal{H}_\infty$ and Nonlinear Approaches*. Hoboken, NJ: Wiley, 2006.

[19] L. Kovács and P. Szalay, "Possibilities and boundaries of $\mathcal{H}_\infty$ control in type 1 diabetes," *In Proc. of 8th IFAC Symposium on Biological and Medical Systems*, pp. 61–66, 2012.

[20] C. M. Ionescu and R. de Keyser, "Relations between fractional-order model parameters and lung pathology in chronic obstructive pulmonary disease," *IEEE T Biomed Eng*, vol. 56, no. 9, pp. 2161–2170, 2011.

[21] C. M. Ionescu, *The human respiratory system. An analysis of the interplay between anatomy, structure, breathing and fractal dynamics*. London: Springer, 2013.